European Radiology (2019) 29:4315–4323
https://doi.org/10.1007/s00330-018-5849-5

CHEST

Dose estimation of ultra-low-dose chest CT to different sized adult patients

Tony M. Svahn[1] · Tommy Sjöberg[2] · Jennifer C. Ast[3]

Received: 19 July 2018 / Revised: 14 September 2018 / Accepted: 22 October 2018 / Published online: 17 December 2018

Abstract

Objectives To evaluate the effect of patient size on radiation dose for standard CT (SD-CT), ultra-low-dose CT (ULD-CT) and two-view digital radiography (DR).

Methods Dosimeters were distributed within the lungs of chest phantoms representing males of 65 kg and 82 kg (body mass indices 23 and 29). In contrast to SD-CT and DR which include automatic exposure control (AEC), the ULD scan employs a fixed mAs value. The phantoms were exposed to SD, ULD and DR while recording lung doses. Projected dose data were calculated from the phantoms. The resulting exposure settings were used in Monte Carlo programs to determine the effective dose for a standard-sized (BMI 24.2) adult male (170 cm/70 kg) and female (160 cm/59 kg). Patients previously examined by both ULD- and SD-CT were identified to determine post hoc size-specific dose estimates (SSDEs).

Results ULD-CT dose was inversely related to patient size; average lung doses summarised in terms of patient size $BMI_{23/29}$ are 5.2/8.1 (SD-CT), 0.56/0.35 (ULD-CT) and 0.05/0.13 mGy (DR), while the effective doses for these techniques on a standard-sized male were 2.9, 0.16 and 0.03 mSv and 2.3, 0.247 and 0.024 mSv for a standard-sized female respectively. SSDEs for 15 patients (averages: BMI 26, range 18–37) averaged 5.5 mGy (3.6–10) for SD-CT and 0.35 mGy (0.42–0.27) for ULD-CT.

Conclusions The effective doses for a standard-sized male and female examined by ULD-CT are (respectively) ~ 6%/~ 11% of SD-CT and ~ 5/~ 10 times higher than DR. ULD-CT gave a lower radiation dosage to larger patients than DR. AEC is warranted in ULD-CT for improved dose consistency.

Key Points

- *For standard-sized patients, ULD-CT dose level is ~ 6%/~ 11% of SD-CT, and ~ 5/~ 10 times higher than DR. For larger patients, ULD-CT is currently being used clinically at lower dose levels than DR.*
- *Using ULD-CT should greatly reduce the risk of late effects from ionising radiation.*
- *AEC in ULD-CT is desirable for increased consistency in patient dose.*

Keywords Tomography · Thoracic radiography · Digital radiography · Radiation dosage

Abbreviations

AEC	Automatic exposure control
ALARA	As low as reasonably achievable
AP	Anterior-posterior
BMI	Body mass index
CTDIvol	Volume CT dose index
DLP	Dose length product
DR	Digital radiography
FOV	Field-of-view
Lat	Lateral
LD	Low dose
mGy	Milligray
mSv	Millisievert
SD	Standard dose
SSDE	Size-specific dose estimate
TLD	Thermoluminescence dosimeter
ULD	Ultra-low dose

This paper was accepted and presented orally at the ECR conference in 2018: Scientific Paper (control number: 3409).

✉ Tony M. Svahn
Tony.Svahn@regiongavleborg.se

[1] Centre for Research and Development, Uppsala University/Region Gävleborg, 801 88 Gävle, Sweden

[2] Department of Surgical Science, Uppsala University, 751 85 Uppsala, Sweden

[3] Department of Organismal Biology, Uppsala University, 752 36 Uppsala, Sweden

Introduction

Chest radiography is one of the most common diagnostic radiological procedures in health care, performed for a wide range of clinical indications. However, because chest radiography is a projection technique, the superimposed anatomy obscures structures of interest [1], and this technique has been shown to be less sensitive to lesions like small parenchymal nodules or small pneumothoraces [2]. Computed tomography (CT) has been proven effective for detecting asymptomatic lung cancer, and has therefore been advocated for as a potential screening tool in place of chest radiography [3]. However, CT delivers a larger radiation dose than most medical imaging techniques, and concerns have grown over the risk to patients of repeated CT imaging. For instance, there has been debate about whether the ionising radiation might increase the risk of developing solid cancers and leukaemia [4], and clearly it is important to further understand the organ dose delivered by CT to help determine the minimum dose possible that still provides sufficient diagnostic information for the radiologist to solve the intended clinical question [5].

To reduce risks of late effects [4], low-dose (LD) CT protocols have been evaluated in recent decades. Early studies of LD scanning generally employed techniques that reduced kVp and/or mAs while performing the image reconstruction using traditional filtered-back projection (FBP) [6]. Reducing slice thickness was shown to improve the detectability of small details, such as calcs; however, this technique also increased image noise [7]. Recently reported average effective doses for LD CT have varied from 1.5 to 2 mSv [8–10], i.e. one sixth to one fourth of conventional chest CT [11]. Modern CT scanners are also equipped with ultra-low-dose (ULD) chest scanning, which has been made possible by advances in various iterative reconstruction (IR) methods, which are much more computationally expensive than FBP and so have only recently become available clinically [12]. The most recent forward projected model-based IR techniques have further decreased the image noise level [12].

At present, very little has been published regarding dosimetry in ULD-CT protocols, and nothing, to the authors' knowledge, that directly compares ULD-CT to both standard CT and radiography. Shaal et al estimated an average effective dose of 0.25 mSv based on exposure data from 55 patients [13], but lack of information about the size of the patients adds uncertainty to this estimate. Current CT scanners display the volume CT dose index and the dose length product, although evaluations using these indicators neglect the patients' body types. To resolve these issues, the American Association of Physicists in Medicine (AAPM) devised the size-specific dose estimate (SSDE) method, a CT index that considers the size of the patient and provides information on the effect of automatic exposure control (AEC) with regard to a suite of patient characteristics [14].

The purpose of the present work is to determine the radiation dose from a readily available clinical protocol of ULD-CT for the chest, and to compare the ULD dose with those from standard CT and digital radiography. To account for various patient sizes, organ dose measurements were performed using differently sized anthropomorphic phantom models, and SSDEs were performed on paired clinical data.

Materials and methods

Phantom models

The multipurpose chest phantom N1 'Lungman' (size 43 × 40 × 48 H cm; Kyoto Kagaku) can be used for both plain radiography and three-dimensional imaging such as CT scanning. The internal components consist of the mediastinum and pulmonary vessels which are attached to an abdominal block (Fig. 1a). This abdominal block is removable, allowing for insertion of tumours and other lesion types as well as dosimeters. The phantom N1 is designed to represent a 168.2-cm tall male weighing 65.4 kg (BMI 23; Fig. 1b), but it is possible to add chest plates of tissue-equivalent material onto the phantom to simulate an overweight adult (82 kg/168.2 cm; BMI 29; Fig. 1c) [15].

Measurements of radiation dose to the lungs

To determine the amount of radiation delivered by the different imaging techniques, the absorbed radiation dose was measured directly by a thermoluminescence dosimeter (TLD) in the Lungman phantom. Prior to use, the TLDs were calibrated according to standard procedures [16]. Twenty TLDs of MCP-N type (LiF:Mg, Cu, P) [16] per lung were placed inside six submillimetre thin acrylic tubes (length 6 cm), separated internally by approximately 2 cm and evenly distributed within the lung parenchyma (Fig. 2). The phantom was exposed to each imaging technique with and without the addition of chest plates. The doses used for scout images were included in the measurements of the CT scans. The TLDs were read using a Harshaw TLD Manual Reader Model 2000 (Thermo Fisher Scientific). In order to minimise detection uncertainties, all examinations were performed ten times and the subsequent readouts were divided ten. Organ doses were assessed by calculating average absorbed doses from the individual TLD dose values. Doses for larger circumferences and higher extrapolated BMIs were calculated assuming the continued linear relationship between dose and circumference/body mass index.

Thoracic CT protocols

An Aquilion Prime CT scanner (Canon Medical Systems) was used for all tests according to protocols given by the manufacturer. On Canon units, the automatic exposure control (SureExposure) adapts the tube current along the longitudinal direction (z) and axial plane (x, y) to account for variations in patient size and density,

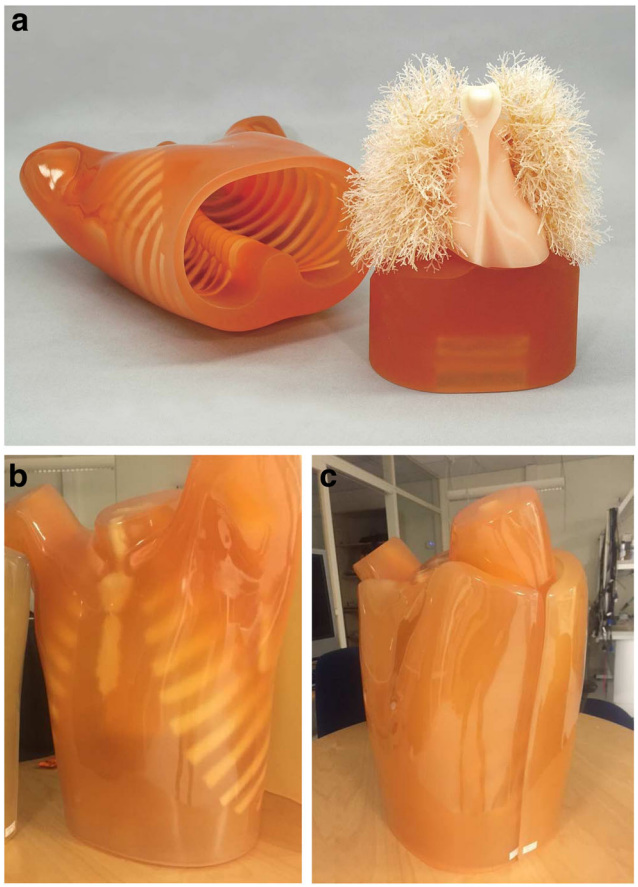

Fig. 1 **a** The abdominal block removed from the Lungman phantom. **b** The torso simulating a male of approximately BMI 23 (chest girth 94 cm). **c** The torso with added chest plates simulating BMI 29 (chest girth 112 cm) [15]

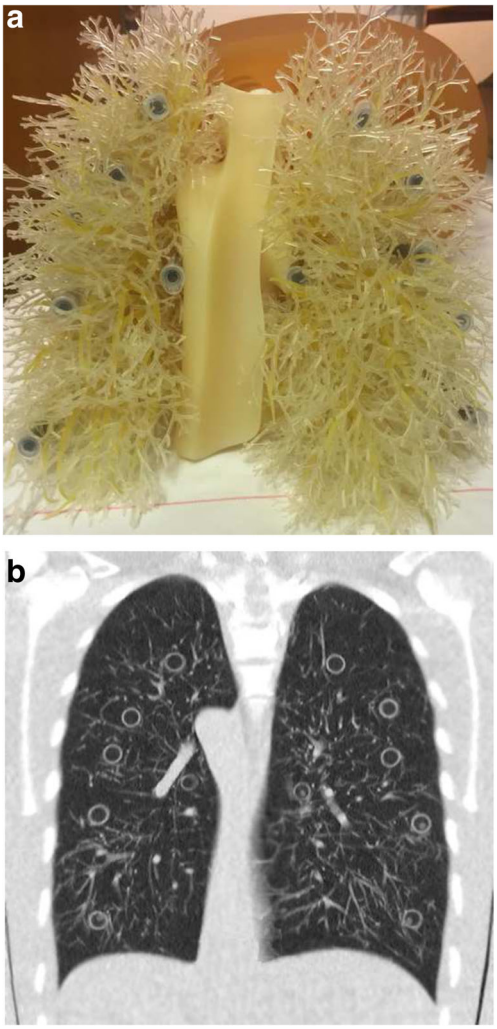

Fig. 2 **a** The Lungman vessels including the TLD arrangements. **b** CT slice of the thorax region indicating the positions of the TLDs

based on the lateral plus frontal scouts, which was the procedure used for standard-CT (SD-CT). The ultra-low-dose CT (ULD-CT) protocol incorporated a fixed tube-current time (mAs). Thus, a frontal scout was acquired at a lower parameter setting (mAs, kVp) that was mainly intended to determine the length of the helical scan. The exposure settings for CT scanning of the phantoms are presented in Table 1.

Digital radiography protocol

Digital chest radiographs were acquired using an Adora DRFi digital X-ray system (Mediel) with a standard local protocol for adults in standing position with automatic exposure control (AEC). The resulting DR parameter settings from exposure of the two phantom sizes are presented in Table 2.

Monte Carlo–based effective dose estimates for a standard-sized patient

Two dedicated Monte Carlo programs were used for computing effective dose, CT-Expo (version 2.5, SASCRAD) for computed tomography, and PCXMC (version 2.0, Finnish Radiation and Nuclear Safety Authority). The latter is often used for imaging modalities that employ 2D geometries [17, 18]; here, it was used for DR. The Monte Carlo computations are performed on mathematical phantoms [19, 20] that include organs at risk in the field-of-view (FOV) as well as scatter contributions to organs outside the FOV. In CT-expo, dose estimates are CT scanner-specific, accounting for beam shape, filter, voltage, geometry and overbeaming; these estimates were applied to the helical scans as well as the CT scouts. The effective dose computations were based on reference persons (adult male, 170 cm/70 kg; adult female, 160 cm/59 kg). For standard CT and DR that had automatic exposure control, the mAs values for a 70 kg patient were estimated by linear regression of those given to patient sizes 65 kg and 82 kg. With the exception of the mAs values, the data presented in Tables 1 and 2 were used in the Monte Carlo effective dose computations using the relevant tissue weights established by the International Commission of Radiological Protection in

Table 1 Thoracic CT protocols

Parameters	Standard CT*¶	Ultra-low-dose CT§¶
Collimation (mm)	80 × 0.5	80 × 0.5
Scanning mode	Helical	Helical
Slice thickness (mm)	5.0	5.0
Pitch	1.388	1.388
Rotation time (s)	0.5	0.35
Tube voltage (kVp)	120	135
Tube current time (mAs: $BMI_{23/29}$)	~49/125	3.5/3.5
Scan length (mm)	349.0	349.0
Orientation	Head first	Head first

*The AP and lateral scout images were acquired with parameter settings 120 kVp, 50 mA and 120 kVp, 30 mA (scan time = 5 s), respectively

§ An AP scout is acquired with parameter settings 80 kVp and 10 mA (scan time = 5 s)

¶ Iterative reconstruction (AIDR-3D)

2007 (i.e. ICRP 103) [21]. For comparison, the doses were also calculated based on the earlier (1990) tissue weights of ICRP 60 [22].

Database search and calculation of size-specific dose estimates

The radiology information system was searched (up until 28 June 2018) to find patients who had been examined by ULD-CT who had also undergone a standard thoracic CT (SD-CT) examination [23]. In addition, SSDEs were also estimated for the two phantoms. The effective diameter of a patient is a circle having an area equal to that of the patient's cross section on a CT image, which can be used as a metric of patient size [14, 24]. From the area of the patient's cross section, the effective diameter was computed as:

$$\text{effective diameter} = \sqrt{\text{AP x LAT}}$$

where the diameter of the patient was measured from a lateral scout (LAT), and from the posterior-anterior scout (PA) using the distance measurement tool available at the SECTRA picture archiving and communication system used at our health care facility. A correction factor is obtained from the AAPM reports 204/220 [14, 24], which is multiplied by the volume CT Dose Index ($CTDI_{vol}$) to obtain the size-specific dose estimate (SSDE). SSDEs were plotted as a function of the size of the patient (i.e. effective diameter) and trend lines were generated using second-order polynomial fits.

Table 2 Digital chest radiography examinations for the different simulated patient thicknesses and imaging projection views

	BMI 23		BMI 29	
	PA	Lateral	PA	Lateral
Tube current time (mAs)	1.7	2.6	3.4	4.5
Tube voltage (kV)	140	140	140	140
Filter combination	1 mm Al, 0.2 mm Cu			
Source-to-image distance (cm)	180			

Results

Dose estimates

Absorbed lung radiation dose and effective dose estimates

Table 3 shows the results of the organ-based absorbed dose measurements for each of the three examination types, including the CT scouts. Depending on the size of the patient, ultra-low-dose (ULD) CT results in an approximately 3 to 12 times higher doses to the lungs than the average dose value for digital radiography (DR), but only 4 to 11% the dose of standard CT (SD-CT). For ULD-CT, the dose was inversely related to patient size and, consequently, the largest dose differences were found for the larger patient size (BMI 29). Since the lateral scout is taken from the left side of the patient in SD-CT, the dose is slightly higher to the left lung. Similarly, being closer to the radiation source in the lateral DR projection, the dose to the right lung was approximately twice that received by the left lung.

The effective doses are shown for a standard-sized male and female (Table 3). Dose contribution from the scouts was 0.31 and 0.39 mSv for a standard-sized male and female, respectively. For ULD, it was 0.01 and 0.02 mSv for a standard-sized male and female (Table 3). The effective doses to a standard-sized patient are based on ICRP 103 [18], while values based on the earlier ICRP 60 [20] tissue-weighting factors are in parenthesis (Table 3). As can be seen, for an adult male, the two reports gave very similar results for each

Table 3 Estimates of the absorbed dose to the lungs for different patient sizes, and effective dose for a standard-sized adult male (170 cm/70 kg) and female (160 cm/59 kg), for standard dose CT (SD-CT), ultra-low-dose CT (ULD-CT), and digital chest radiography (DR; PA + LAT views). The estimates include dose contributions from the CT scouts

	Radiation dosage for complete examinations							
	Absorbed dose to the lungs (mGy)						Effective dose (mSv)[¶*]	
	BMI 23			BMI 29			BMI 24.2	BMI 23
	Left lung	Right lung	Average	Left lung	Right lung	Average	Male, ♂	Female, ♀
SD-CT	5.4	4.9	5.2	8.24	7.95	8.1	2.9 (2.8)	2.3 (1.8)
ULD-CT	0.57	0.55	0.56	0.34	0.36	0.35	0.16 (0.15)	0.247 (0.2)
DR	0.032	0.06	0.046	0.08	0.18	0.13	0.03 (0.03)	0.024 (0.021)

[¶] Effective dose assessment was performed using PCXMC for DR and CT-EXPO for CT

*Effective dose computations were based on the recent ICRP 103 report (estimates based on the ICRP 60 report in parentheses)

type of examination, while for females, the differences are somewhat larger, possibly due to differences in tissue weights for breasts (i.e. the tissue-weighting factor in ICRP 103 is 0.12, and 0.05 in ICRP 60) [21, 22].

Projected organ doses

The average organ dose data recorded from the phantoms (Table 3) indicate that, for larger-sized patients (with circumferences approximately > 125 cm), the ULD protocol operates at lower dose levels than DR (Fig. 3a). A correspondingly sized phantom would have approximately BMI > 33 (> 95 kg, 168.2 cm; male) (Fig. 3b).

Patient population, dose indicators and size-specific dose estimates derived from their examinations

Fifteen patients (six females and nine males) were found that had undergone examinations with both CT techniques. Their average weight was 76 kg (range 53–120 kg) registered at the time of the SD-CT examination and their average height was 174 cm (range 160–182 cm; avg. BMI 26 (range 18–37). In 12 cases, the different types of examinations were performed within 3 months of each other; in three cases, they were performed within the same year. CTDIvol averaged 5.59 mGy (1.4–2.8) for SD-CT and fixed at 0.3 mGy for ULD-CT, whereas dose length products averaged 203 mGycm^2 (85–429) for SD-CT and 9.7 mGycm^2 (7.5–12.3) for ULD-CT. SSDEs averaged 5.5 mGy (3.6–10) for SD-CT and 0.35 mGy (0.42–0.27) for ULD-CT. The volume CT dose index (CTDIvol) of ULD-CT was constant, while it had an upward curvature for SD-CT (Fig. 4a). A correction factor is applied to the CTDIvol to obtain the SSDE. The effect of adjusting for patient size can be visualised by comparing Fig. 4a and b. In comparison to CTDIvol, the SSDE typically diminished for larger patients, but elevated for smaller patients. The ULD-CT dose decreased linearly with patient size (effective diameter), while the SSDE for SD-CT was much more variable and showed a stronger upward curvature with patient size (Fig. 4b). The phantom-based SSDEs were close to or on the trend lines for patients.

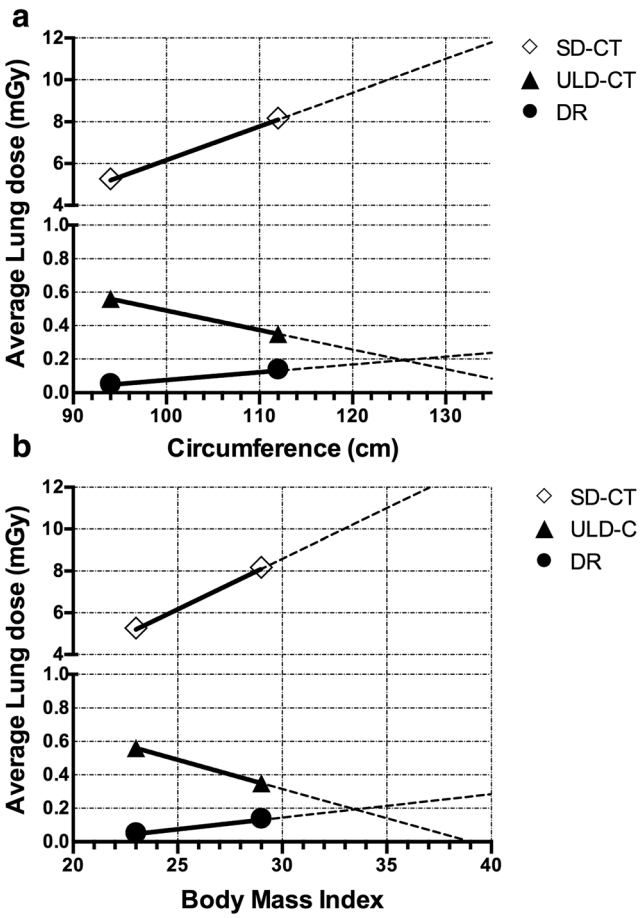

Fig. 3 The average doses to the lungs as a function of (**a**) circumference, and (**b**) extrapolated body mass index. The dashed lines are projections of the measured data

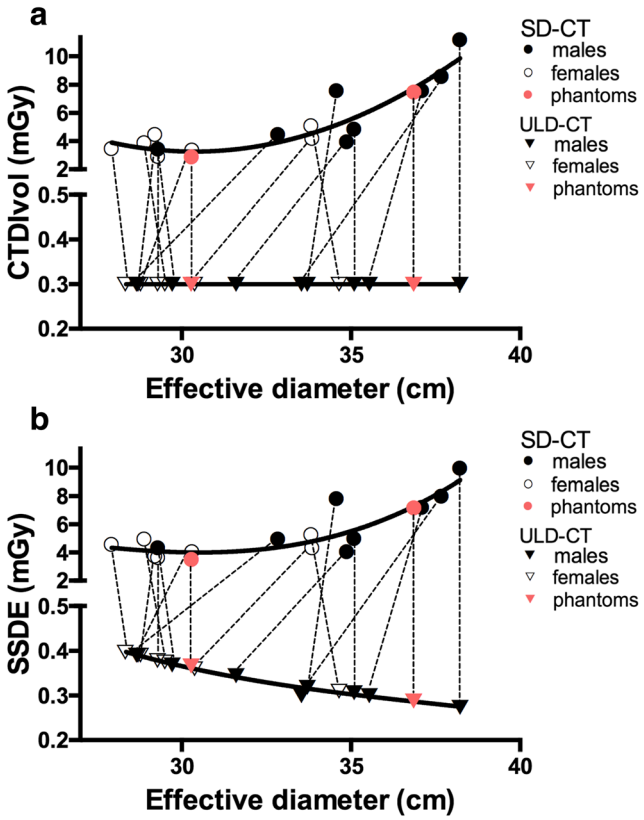

Fig. 4 **a** The volume CT dose index (mGy) and (**b**) size-specific dose estimates (mGy) for standard dose CT (circles) and ultra-low-dose CT (triangles) protocols for paired patient cases. SSDEs for the Lungman phantoms (BMI 23 and 29) are indicated in red. Note the break in the vertical axes

Discussion

The principle of ALARA ('as low as reasonably achievable') introduced by the International Commission of Radiological Protection (ICRP) has become more relevant in this era of increased use of CT for diagnostic and interventional procedures, and efforts should be made to reduce unnecessary radiation exposure from CT [22]. Calculated effective doses and size-specific dose estimates (SSDE) both showed that ULD-CT delivered only about 6 to 7% of the radiation dose for SD-CT to a standard-sized patient, or approximately only approximately four to five times more than digital radiography (DR). In these tests, DR yielded the lowest effective dose of the evaluated imaging modalities (0.024–0.03 mSv for a standard-sized patient), although it should be noted that this dose was lower than some previously reported effective doses for DR (ranging from 0.027–0.1 mSv) [25]. As suggested by the projected doses (Fig. 3), ULD-CT is currently being used clinically at lower radiation dose levels than DR for larger-sized patients.

The particular ULD-CT protocol used here was recently evaluated for screening of asbestos-related pleuropulmonary diseases [13]. Diagnostic accuracy of ULD-CT was high for the primary endpoint (sensitivity = 90.9%, specificity = 100%, positive predictive value = 100%, negative predictive value = 97.8%), and ULD-CT was therefore suggested as a suitable first-line screening test to be complemented by SD-CT only in doubtful or apparently positive cases [13]. Previously, low-dose CT examinations were able to demonstrate parenchymal lung manifestations in a higher-risk asymptomatic sub-group of asbestos-exposed patients, and showed potential for lung cancer screening in this specific population [26, 27]. However, these low-dose examinations had effective doses around 1.5 to 2 mSv. These estimates were at the time (between 2000 and 2010) considered to be low doses, but are 6 to 13 times higher than our estimates for ULD-CT, and not that much lower than the current SD-CT protocol.

The SD-CT protocol evaluated in the current study was roughly two-fifths the dose of conventional chest CT (7–8 mSv), showing that the radiation dose in standard chest CT protocols has in fact also decreased. Typically, total scanning time is shorter in newer models of CT scanners. For instance, both CT protocols used here incorporated a 'fast' pitch of 1.39, which reduces blurring effects caused by patient motion. However, the majority of the radiation dose difference between the two CT protocols results from the different tube currents (Table 1).

The ULD-CT effective dose (0.16 mSv) was comparable to that recently reported for chest tomosynthesis for a standard-sized adult male (0.13 mSv) [28, 29]. Tomosynthesis works by collecting low-dose projections at a limited angular range, and then using these projections to reconstruct section images [30]. Because this technique uses flat-panel detectors, it has a high in-plane resolution. CT has more complete image sampling, offering isotropic resolution and further decreased structural 'noise' from superimposed anatomy, which for instance allows for novel applications such as semi-automatic 3D volumetric nodule measurements of growth [31]. Recent advances in CT techniques include improvements regarding the focal spot size which increase the in-plane resolution [32, 33], often referred to as 'super resolution'. Consequently, it will be highly relevant and very interesting to compare the two techniques in terms of clinical performance.

Not surprisingly, the SSDEs of real patients were more variable than projected doses based on measurements in the anthropomorphic phantom (Fig. 4), but certain trends within the automatic exposure control (AEC) can still be observed. Because tube current was kept fixed during the scan without regard to the size of the patient, the ULD protocol yielded low variability in SSDEs. In contrast, there was a greater variability in SSDEs for SD-CT, and a tendency for dose to increase more rapidly with increased patient size. The variability might be explained by inclusion or exclusion of arms and/or breasts in the scout images, which affects the AEC and the correlation of data points. Using AEC during radiological examinations will typically require increased exposure for patients with larger chest circumferences in order to maintain image quality.

The incremental effect in SSDEs with increasing patient size might be due to a higher proportion of fatty tissue in these patients, which would increase both the amount of scattered radiation and the image noise level, which would in turn have to be compensated for with a higher dose. The variability seen for SD-CT was probably also enhanced by the fact that dose itself was at a higher level than ULD-CT (i.e. variability simply becomes more pronounced with higher doses).

In a few cases, a patient's estimated size (effective diameter) was considerably different for the SD- and ULD-CT scans (Fig. 4). Despite this variation, the fact that the dose values were still close to or on the trend lines for the entire group demonstrates that SSDE is making allowances for differences in estimated patient size. No obvious differences were seen between SSDEs for females and males; however, the sample is too small to subdivide into a study of such effects. The fact that the SSDEs of the phantoms fit very well with the patient-derived data provides a proof-of-utility of the phantoms for dosimetry. A more accurate measure of true patient size could potentially be derived from the data from the helical scans. Although this method is not current standard practice, it would be interesting to evaluate in a large-scale study.

When using a fixed mAs value, the ULD protocol is usually thought to yield relatively lower quality images (because of the lower radiation dose) for larger-sized patients than for smaller ones. Even though it is encouraging that the protocol operates at lower dose levels than DR for some patients, the fact that variable image quality and/or patient doses are being generated for different patient types is suboptimal. Relating image quality to patient size to determine a sufficient dose level with regard to image quality was however beyond the scope of the current work. In future work, if possible, it would be desirable to determine an appropriate noise level to be set in the AEC for maintaining image quality for different types of patients.

Utilising an AEC requires proper quality of the CT scouts. In ULD-CT, a slight increase in radiation dosage may be necessary to enable dose modulation by performing a lateral CT scout. For the settings used in the frontal scout, the effective dose would only increase by approximately 0.01–0.02 mSv. It is noteworthy that the dose of the SD-CT scouts was as much as twice that of the complete ULD-CT examination. The optimal parameter settings required for proper modulation remains to be evaluated. An alternative approach would be to adjust the scan parameters in the helical scan according to weight-classes, which could be evaluated in phantoms studies and would not require any additional scout-related radiation to patients.

Because ULD-CT methods expose patients to less radiation than conventional methods and have higher diagnostic accuracy than 2D imaging, these scans have already replaced traditional radiology for a number of diagnostic procedures [10, 34, 35], and might be especially appropriate for younger patients who are more sensitive to radiation [21]. Furthermore, several recent studies have suggested promising new applications for these examinations [7, 12, 13]. Unfortunately, many radiology departments have not been able to meet the increased demand for CT scans. Making the transition from traditional techniques to CT systems will require significant financial investment in equipment, building and room design and staff recruitment and training [36]. The cost effectiveness of such a transition has not been studied. ULD-CT technology offers the potential to optimise doses, and additional refinements in ULD technology (such as image reconstruction and optimised automatic exposure controls) will allow for further dose savings. Ongoing and new studies of ULD-CT in the screening setting in particular should monitor and report absorbed dose levels to inform future screening practice and policy. The ULD-CT method is new and still being developed, but it is clearly worthy of further research to ensure its adoption into routine practice, and we hope that this study contributes a positive step in that development.

A limitation of this study is that the TLDs have an inherent uncertainty in sensitivity (< 7%). However, the use of a large number of dosimeters (20) for each lung and multiple exposures per examination should help ensure that the average doses reported here are accurate.

In conclusion, the effective dose for ultra-low-dose (ULD) CT for standard-sized patients is ~ 6%/~ 11% of standard (SD) CT. For larger patients, ULD-CT delivers a lower radiation dose than digital radiography (DR). ULD chest CT may serve as a good alternative for both SD-CT and conventional DR, considerably reducing the effective radiation dose required by SD-CT while elevating diagnostic accuracy over DR. Increased awareness of the ULD protocol may lead to increased clinical CT usage at local health care centres and smaller radiology departments.

Acknowledgements The authors would like to thank Prof. Hans Dieter Nagel at the Science & Technology for Radiology, Germany; Dr. Teemu Siiskonen, at the Finnish Radiation Authority (STUK); and Dr. Yoko Kagaku, Kyoto Kagaku Co., Ltd., for their support and assistance with this project.

Funding The authors state that this work has not received any funding.

Compliance with ethical standards

Guarantor The scientific guarantor of this publication is Tony Martin Svahn.

Conflict of interest The authors of this manuscript declare no relationships with any companies, whose products or services may be related to the subject matter of the article.

Statistics and biometry One of the authors has significant statistical expertise.

No complex statistical methods were necessary for this paper.

Informed consent Written informed consent was not required for this study because only exposure data and parameter settings were extracted from examinations in retrospect, in addition to phantom data.

Ethical approval Institutional Review Board approval was not required because for this study because only exposure data and parameter settings were extracted from examinations in retrospect, in addition to phantom data.

Methodology
- Retrospective
- Observational and experimental
- Performed at one institution

References

1. Båth M, Håkansson M, Börjesson S et al (2005) Nodule detection in digital chest radiography: effect of anatomical noise. Radiat Prot Dosimetry 114(1–3):109–113
2. Blanchon T, Bréchot JM, Grenier PA et al (2007) Baseline results of the Depiscan study: a French randomized pilot trial of lung cancer screening comparing low dose CT scan (LDCT) and chest X-ray (CXR). Lung Cancer 58(1):50–58
3. Terra-Filho M, Bagatin E, Nery LE et al (2015) Screening of miners and millers at decreasing levels of asbestos exposure: comparison of chest radiography and thin-section computed tomography. PLoS One 10(3):e0118585
4. National Research Council (2006) Health risks from exposure to low levels of ionizing radiation: BEIR VII phase 2. The National Academies Press, Washington, DC, p 245
5. International Commission on Radiological Protection (1975) Report of the Task Group on Reference Man. ICRP Publication 23. Pergamon Press, Oxford Adopted October 1974
6. Zhu X, Yu J, Huang Z (2004) Low-dose chest CT: optimizing radiation protection for patients. AJR Am J Roentgenol 183(3): 809–816
7. Ketelslegers E, Van Beers BE (2006) Urinary calculi: improved detection and characterization with thin-slice multidetector CT. Eur Radiol 16(1):161–165
8. Kubo T, Ohno Y, Nishino M et al (2016) Low dose chest CT protocol (50 mAs) as a routine protocol for comprehensive assessment of intrathoracic abnormality. Eur J Radiol Open 3:86–94
9. Rampinelli C, De Marco P, Origgi D et al (2017) Exposure to low dose computed tomography for lung cancer screening and risk of cancer: secondary analysis of trial data and risk-benefit analysis. BMJ 356:j347
10. Larke FJ, Kruger RL, Cagnon CH et al (2011) Estimated radiation dose associated with low-dose chest CT of average-size participants in the National Lung Screening Trial. AJR Am J Roentgenol 197(5):1165–1169
11. Mettler FA Jr, Huda W, Yoshizumi TT, Mahesh M (2008) Effective doses in radiology and diagnostic nuclear medicine: a catalog. Radiology 248(1):254–263
12. Fujita M, Higaki T, Awaya Y et al (2017) Lung cancer screening with ultra-low dose CT using full iterative reconstruction. Jpn J Radiol 35(4):179–189
13. Schaal M, Severac F, Labani A, Jeung MY, Roy C, Ohana M (2016) Diagnostic performance of ultra-low-dose computed tomography for detecting asbestos-related pleuropulmonary diseases: prospective study in a screening setting. PLoS One 11(12):e0168979
14. Brady SL, Kaufman RA (2012) Investigation of American Association of Physicists in Medicine report 204 size-specific dose estimates for pediatric CT implementation. Radiology 265(3):832–840
15. Kyoto Kagaku Ltd. Multipurpose chest phantom N1 "LUNGMAN". http://www.kyotokagaku.com/products/detail03/ph-1.html. Accessed 27 Oct 2018
16. Shrimpton PC, Jones DG, Hillier MC, Wall BF, Le Heron JC, Faulkner K (1991) Survey of CT Practise in the UK. Part 2: dosimetric aspects (NRPB-R249). National Radiological Protection Borard, Chilton
17. Stamm G, Nagel HD (2002) CT-expo–a novel program for dose evaluation in CT. Rofo 174(12):1570–1576
18. Tapiovaara M, Lakkisto M, Sermovaa A (1997) PCXMC: a PC-based Monte Carlo program for calculating patient doses in medical x-ray examinations. Finnish Centre for Radiation and Nuclear Safety, Helsinki
19. Cristy M, Eckerman K (1987) Specific absorbed fractions of energy at various ages from internal photon sources. Parts I-VII (ORNL/TM-8381). Oak Ridge National Laboratory, Oak Ridge, pp 1–74
20. Zankl M, Panzer W, Drexler G (1991) The calculation of dose from external photon exposures using reference human phantoms and Monte Carlo methods. VI. Organ doses from computed tomographic examinations. GSF-Forschungszentrum für Umwelt und Gesundtheit, Institut für Strahlenschutz, Neuherberg
21. International Committee on Radiological Protection (2007) The 2007 Recommendations of the International Commission on Radiological Protection. ICRP publication 103. Ann ICRP 37(2–4):1–332
22. International Committee on Radiological Protection (1991) 1990 Recommendations of the International Commission on Radiological Protection. ICRP publication No. 60. Pergamom, Oxford
23. Rubin DL (2011) Informatics in radiology: measuring and improving quality in radiology: meeting the challenge with informatics. Radiographics 31(6):1511–1527
24. McCollough C, Bakalyar DM, Bostani M et al (2014) Use of water equivalent diameter for calculating patient size and size-specific dose estimates (SSDE) in CT: the report of AAPM task group 220. AAPM Rep 2014:6–23
25. Weatherburn GC, Bryan S, Davies JG (2000) Comparison of doses for bedside examinations of the chest with conventional screen-film and computed radiography: results of a randomized controlled trial. Radiology 217(3):707–712
26. Fasola G, Belvedere O, Aita M et al (2007) Low-dose computed tomography screening for lung cancer and pleural mesothelioma in an asbestos-exposed population: baseline results of a prospective, nonrandomized feasibility trial—an Alpe-Adria thoracic oncology multidisciplinary group study (ATOM 002). Oncologist 12(10): 1215–1224
27. Carrillo MC, Alturkistany S, Roberts H et al (2013) Low-dose computed tomography (LDCT) in workers previously exposed to asbestos: detection of parenchymal lung disease. J Comput Assist Tomogr 37(4):626–630
28. Båth M, Svalkvist A, von Wrangel A, Rismyhr-Olsson H, Cederblad A (2010) Effective dose to patients from chest examinations with tomosynthesis. Radiat Prot Dosimetry 139(1–3):153–158
29. Dobbins JT 3rd, McAdams HP, Sabol JM et al (2017) Multi-institutional evaluation of digital tomosynthesis, dual-energy radiography, and conventional chest radiography for the detection and management of pulmonary nodules. Radiology 282(1):236–250
30. Lång K, Andersson I, Rosso A, Tingberg A, Timberg P, Zackrisson S (2016) Performance of one-view breast tomosynthesis as a stand-alone breast cancer screening modality: results from the Malmo

Breast Tomosynthesis Screening Trial, a population-based study. Eur Radiol 26(1):184–190
31. Han D, Heuvelmans MA, Oudkerk M (2017) Volume versus diameter assessment of small pulmonary nodules in CT lung cancer screening. Transl Lung Cancer Res 6(1):52–61
32. Alvare G, Gordon R (2017) Foxels for high flux, high resolution computed tomography (foxelct) using broad x-ray focal spots: Theory and two-dimensional fan beam examples. Radiol Diagn Imaging 1(1):1–40
33. Oyama A, Kumagai S, Arai N et al (2018) Image quality improvement in cone-beam CT using the super-resolution technique. J Radiat Res 59(4):501–510
34. Naidu SG, Kriegshauser JS, Paden RG, He M, Wu Q, Hara AK (2014) Ultra-low-dose computed tomographic angiography with model-based iterative reconstruction compared with standard-dose imaging after endovascular aneurysm repair: a prospective pilot study. Abdom Imaging 39(6):1297–1303
35. Rob S, Bryant T, Wilson I, Somani BK (2017) Ultra-low-dose, low-dose, and standard-dose CT of the kidney, ureters, and bladder: is there a difference? Results from a systematic review of the literature. Clin Radiol 72(1):11–15
36. Thurley P, Crookdake J, Norwood M, Sturrock N, Fogarty AW (2018) Demand for CT scans increases during transition from paediatric to adult care: an observational study from 2009 to 2015. Br J Radiol 91(1083):20170467